Journal of Traditional and Complementary Medicine 13 (2023) 600–610

Contents lists available at ScienceDirect

Journal of Traditional and Complementary Medicine

journal homepage: http://www.elsevier.com/locate/jtcme

Xiaozheng pill exerts an anti-mammary hyperplasia effect through Raf/ERK/ELK and HIF-1α/bFGF pathways

Yu-fei Liu [a, b, 1], Tian An [c, 1], Hong Yu [a], Ying-yi Fan [a, *], Xiao-hua Pei [a, d, **]

[a] Beijing University of Chinese Medicine Third Affiliated Hospital, Beijing, China
[b] Department of General Surgery, Tsinghua University Yuquan Hospital, Beijing, China
[c] School of Traditional Chinese Medicine, Capital Medical University, Beijing, China
[d] Xiamen Hospital, Beijing University of Chinese Medicine, Xiamen, China

ARTICLE INFO

Article history:
Received 23 September 2022
Received in revised form
16 April 2023
Accepted 30 May 2023
Available online 7 June 2023

Keywords:
Hyperplasia of mammary glands
Xiaozheng pill (XZP)
Angiogenesis
Apoptosis
Metabolomics

ABSTRACT

Background and aim: The purpose of this study is to explore whether the Xiaozheng pill (XZP) has the effect of anti-hyperplasia of mammary glands (HMG) and to identify the related signaling pathways.
Experimental procedure: We analyzed the effective chemical components of the XZP, as well as the key chemical components, key proteins, main biological processes, and pathways in the treatment of HMG; Secondly, the levels of Estradiol (E2), Follicle-stimulating hormone (FSH), Luteinizing hormone (LH), Progesterone (P), Raf/ERK/ELK and HIF-1α/bFGF pathways related proteins were detected; Finally, the effect of XZP on metabolites was analyzed by metabolomics.
Results and conclusion: In this study, we identified key targets and pathways for XZP therapy of HMG, including EGFR, VEGFA, ER, and Ras signaling pathways. Animal experiments show that XZP can reduce the levels of E2, LH, and FSH and increase the expression of P in HMG mice. XZP can restore the normal structure of breast tissue and reduce ERα, ERβ, and PR expression in breast tissue. In addition, metabolomics results show that XZP also regulates HMG metabolites, including HIF-1α and metabolic pathways. The Western blot results showed that XZP intervention can reduce the protein expression of *p*-Raf1, Raf1, *p*-ERK1/2, ERK1/2, ELK, HIF-1α, and bFGF in the breast tissue of HMG mice. XZP may eliminate abnormal breast hyperplasia through inhibition of apoptosis and angiogenesis, which may be linked with the regulation of the Raf/ERK/ELK and HIF-1α/bFGF signaling pathways in HMG mice. These results suggest that XZP treatment may be beneficial for the management of HMG.
© 2023 Center for Food and Biomolecules, National Taiwan University. Production and hosting by Elsevier Taiwan LLC. This is an open access article under the CC BY-NC-ND license (http://creativecommons.org/licenses/by-nc-nd/4.0/).

1. Introduction

Hyperplasia of mammary glands (HMG), also known as cystic hyperplasia, lobular hyperplasia, or structural dysplasia of mammary gland, is closely related to mammary ducts, fibrous tissue, or acinus hyperplasia.[1,2] The incidence rate of HMG in China is about 40%, which is mainly found in 25-to 45-year-old women and accounts for >70% of all breast diseases that occur among middle-aged women.[3,4] The main manifestations of HMG are breast pain and breast lumps, or nipple discharge.[5] Researchers have identified that the periodic imbalance of progesterone (P) and estrogen (E2) levels and the stimulation of E2 on breast tissue are the principal reasons for the occurrence of HMG.[6] HMG is closely related to breast cancer, and its cumulative canceration rate of HMG in 7 years is about 9.9%.[7,8] With the incidence rate of HMG increasing year by year, the early diagnosis and treatment of HMG are extremely important and have positive significance in preventing breast cancer.[9,10] Nevertheless, the exact mechanism and etiology of triggering these key hormone and metabolic disorders of HMG remain largely unknown. In the last decade, metabolomics has been extensively used in the study of disease-related metabolites, which provides an important contribution to the study of metabolic diseases.[11]

* Corresponding author.
** Corresponding author. Xiamen Hospital, Beijing University of Chinese Medicine, Xiamen, China.
E-mail addresses: fan38898901@126.com (Y.-y. Fan), pxh_127@163.com (X.-h. Pei).
Peer review under responsibility of The Center for Food and Biomolecules, National Taiwan University.
[1] Yu-fei Liu and Tian An have contributed equally to this work.

https://doi.org/10.1016/j.jtcme.2023.05.002
2225-4110/© 2023 Center for Food and Biomolecules, National Taiwan University. Production and hosting by Elsevier Taiwan LLC. This is an open access article under the CC BY-NC-ND license (http://creativecommons.org/licenses/by-nc-nd/4.0/).

In recent years, traditional Chinese medicine (TCM) has gradually become the first choice for the treatment of HMG because of its exact curative effect and high safety.[12] As a TCM formula for the treatment of HMG in clinical practice for many years, the Xiaozheng pill consisted of 11 herbal medicines, including *Radix Bupleuri, Cyperi Rhizoma, Radix Rhei Et Rhizome, Citri Reticulatae Pericarpium Viride, Chuanxiong Rhizoma, Curcumae Rhizoma, Ground Beetle, Fritillariae Thunbrgii Bulbus, Angelicae Sinensis Radix, Paeoniae Radix Alba, Vaccariae Semen*. The chemical composition of XZP has been elucidated in 11 batches of XZP drugs through high-performance liquid chromatography and mass spectrometry techniques in early studies.[13] Previous clinical studies have proved that the XZP has a good therapeutic effect on HMG, and the total effective rate is 86.43%.[14] After treatment with XZP, the size, and distribution of breast mass gradually reduced, and the hardness of the mass decreased.[15] As a new research method, metabolomics has attracted more and more attention in recent years.[16] In metabolomics research, metabolite analysis can be used to determine metabolites and physiological states, and ultimately understand the potential biological mechanism.[17,18] However, based on metabolomics data, there is still a lack of a rapid evaluation of the potential of XZP.

Previous studies have confirmed the clinical efficacy of XZP, but its potential anti-HMG mechanism and related pathways remain unclear. Therefore, we established a mouse model of HMG based on estradiol benzoate and progesterone to investigate the protective effect and its mechanism of XZP on estrogen-induced HMG. In addition, quantitative methods were used to investigate the effect of XZP on the expression of endogenous small molecule metabolites in HMG models and to explore the effect of XZP on estrogen-induced metabolites in HMG mice.

2. Methods and materials

2.1. Network pharmacology analysis of XZP in treating HMG

2.1.1. Screening and target prediction of active components in XZP

We refer to the previous network pharmacology research methods for operation,[19] in particular, all the ingredients in XZP were obtained through two databases: TCMSP (https://tcmspw.com/tcmsp.php), and TCMID (http://119.3.41.228:8000/tcmid/). The related active components were screened by oral bioavailability (≥30%) and drug-likeness (≥0.18). Then, the relationship network between traditional Chinese medicine and its active components in XZPs was constructed by using the software of Cytoscape 3.6.0. In addition, the TCMSP platform and PubChem database were used for searching the corresponding targets of active ingredients in XZPs. Ultimately, target gene information was standardized through the UniProt website (https://www.uniprot.org/), and genes without UniProt ID of human samples was eliminated.

2.1.2. Screening of key targets of XZP in treating HMG

With "hyperplasia of mammary glands" as the keyword, we searched in the OMIM (https://omim.org/) and GeneCards database (https://www.genecards.org/). Then we combined the results and standardized the gene information through the UniProt website to construct the target data set of breast hyperplasia. Through Venny 2.1.0, the corresponding targets of active ingredients in XZPs were integrated with HMG targets to construct Venn Diagram. Subsequently, the protein-protein interaction (PPI) figure of the corresponding targets of active components of XZP and HMG disease targets was constructed online using the STRING database (https://www.string-db.org/), and the topological analysis was further carried out by Cytoscape 3.6.0 software.

2.1.3. Gene functional analysis of drug targets and HMG disease targets in XZP

Bioinformatics analysis was used to analyze the gene function of the corresponding target of XZP and the common target of HMG disease. Specifically, the DAVID Database (https://david.ncifcrf.gov/) was used for target gene ontology (GO) analysis, and the Kyoto Encyclopedia of Genes and Genomes (KEGG) for signal pathway enrichment analysis. Using $P < 0.05$ as the screening criteria, the biological process (BP) and KEGG signaling pathway were obtained.

2.2. Efficacy and mechanism of XZP in treating HMG in mice

2.2.1. Animals and treatments

C57BL/6JNifdc female mice (6–8 weeks) were obtained from Beijing Vital River Laboratory Animal Technology Co., Ltd. (Beijing, China). The mice were housed in the specific pathogen-free (SPF) environment at the Beijing University of Chinese Medicine (BUCM) with free access to water and chow. All operations in this study were approved and reviewed by the Animal Care Committee of BUCM.

C57BL/6JNifdc mice were randomly divided into the normal group (NC, n = 15), HMG model control group (HMG, n = 15), Tamoxifen group (Tam, n = 15), XZP high-dose group (XZH, n = 15), XZP medium-dose group (XZM, n = 15), and XZP low-dose group (XZL, n = 15). Except for the normal group, the other groups refer to the 2017 Chinese Society of TCM published "mammary gland hyperplasia animal model preparation specification": establish HMG model by intraperitoneal injection of estradiol benzoate and progesterone.[20] Then, according to the human and animal drug dose conversion coefficient table,[21] the drug was administered by gavage. The mice in the Tam group were daily administrated with Tam at a dosage of 3.9 μg/g/d by gavage. The mice in XZH, XZM, and XZL groups were daily gavaged with 1.8, 0.9, and 0.45 mg/g/d of XZP, respectively. The mice in HMG and NC groups were orally administrated with an equal volume of distilled water. All the mice were gavaged continuously for 30 days.

2.2.2. Effect of XZP on organ index and hormone in HMG mice

2.2.2.1. Organ index and serum hormone analysis. After 30 days of intervention, the mice were weighed before being euthanized, and the breasts, spleen, liver, kidney, uterus, and accessories of mice in each group were extracted. The weight of each organ was measured and recorded, and the organ index was calculated[22]:

$$\text{Organ index} = (W_{organ} \times 10)/ W_{body}$$

We randomly selected 9 mice from each group for serum hormone analysis. The blood samples were collected by the eyeball extraction method and then centrifuged at 3000r/min to separate the serum, which was stored for subsequent experiments. Serum levels of luteinizing hormone (LH), E2, P, and follicle-stimulating hormone (FSH) were measured by ELISA (ImmunoWay, USA).

2.2.2.2. H&E staining of liver and breast in HMG mice. Liver and breast tissues were immersed in 10% neutral formalin for 3 days, and further dehydration and transparency with different concentrations of ethanol (50–100%) and xylene.[23] Then they were embedded in paraffin overnight and sectioned of ~5-μm thickness for the H&E staining. Subsequently, the Olympus bx53 scanning system (Tokyo, Japan) was used for the histopathological examination of liver and breast tissue sections, including the structure and morphology of the acinar cavity and duct in the breast. In addition, the liver tissue was also evaluated to further verify the safety of the XZP.

2.2.2.3. Metabolomics analysis of XZP in treating HMG mice. We randomly selected 6 mice from each group for serum metabolomics analysis. First, we centrifuged the blood samples of each mouse for 10 min (5000 rpm, 4 °C) to obtain the serum. Furthermore, methanol was added to each sample at a ratio of 1:3 (V/V), and the protein was obtained by rotating for 10 min and centrifuging for 15 min (10000 rpm, 4 °C). The supernatant was then transferred to a clean centrifuge tube and dried at 40 °C under mild nitrogen flow. Finally, 200 μ L methanol was used to recombine the dried residue for metabolomics analysis. Briefly speaking, we used Thermo Scientific Dionex Ultimate 3000 UHPLC plus for metabolomics analysis. All analyses were equipped with a 2.1 × 100 mm BEH 1.7 μ M C18 column. According to previous studies, biomarkers were screened.[24] By setting parameters: injection volume 2 μ 50. Flow rate 230 μ The column temperature was 30 °C. The mobile phases were 0.1% formic acid aqueous solution (a) and 0.1% formic acid acetonitrile solution (b). To collect metabolites. Finally, the metabolomics data were collected by Fourier transform high-resolution full scan.

2.2.2.4. Immunohistochemical staining of breast tissue in HMG mice. Immunohistochemical (IHC) staining was done according to the instructions on the kits. Briefly, 5-μm sections of demineralized and paraffin-embedded breast were kept in the oven at 60 °C for 4 h and sequentially treated with xylene, descending graded ethanol (100-70%), antigen retrieval solution (ZSGB-BIO, Beijing, China), and 3% H2O2 (30 min). Then, the slides were rinsed and incubated with a primary antibody [ERα (1:400), ERβ (1:50), PR (1:300), PBS (1:50)] at 4 °C. For the negative controls, the primary antibody was replaced by nonimmunized goat serum. Fifteen hours later, the slides for IHC staining were rinsed and incubated with the corresponding secondary antibodies (Proteintech, USA) for 1 h followed by DAB and hematoxylin staining, respectively. Finally, the slides were examined and photographed using an Olympus BX53 microscope (Tokyo, Japan) and analyzed by Image software.

2.2.2.5. Western blot analysis. After the mice sacrifice, the breast tissue was homogenized and extracted in RIPA buffer containing a protease inhibitor cocktail (R0020, Solarbio, Beijing, China), and the protein concentration was determined by a BCA kit (BC3710, Solarbio, Beijing, China). A total of 20 μL breast protein samples were separated by 10% SDS-PAGE electrophoresis and then transferred onto a PVDF membrane at 100 V for 60 min (Bio-Rad, USA). After being blocked with 5% skimmed milk in TBST for 1 h at room temperature, the PVDF membranes were then incubated with the appropriate primary antibodies [HIF-1α (1:500, ab1, Abcam, USA), Raf1 (1:1,000, ab50858, Abcam, USA), bFGF (1:1,000, 05–118, Millipore, USA), *p*-Raf1 (1:1,000, ab173539, Abcam, USA), *p*-ERK1/2 (1:1,000, ab201015, Abcam, USA), ERK1/2 (1:1,000, 16443-1-AP, Proteintech, USA), ELK (1:1,000, ab32106, Abcam, USA)] overnight at 4 °C. The next day, after rinsing the PVDF membrane with TBST for 30 min, and then PVED membranes were incubated with the corresponding horseradish peroxidase-labeled secondary antibody (1:1,000, KGAA35, KeyGEN, China) at room temperature for 2 h. Positive bands were visualized with enhanced chemiluminescence liquid and quantified using the Image J software. GAPDH (1:1,000, ab181602, Abcam, USA) as the internal control.

2.3. Statistical analysis and metabolomics data analysis

This study used GraphPad Prism 8.1 software to analyze the data. All results were expressed as mean ± SD. When the homogeneity and normality of variance are satisfied, one-way ANOVA is used to evaluate the data in multiple groups. If not, Dunnett's T3 and nonparametric tests were performed. $P < 0.05$ was considered statistically significant. In addition, the original data of metabolomics were analyzed using the version 2.1 software package. Using SIMCA-P13.0 software to conduct principal component analysis. Furthermore, the cluster analysis of different metabolites was performed by using the multi-experiment viewer (V4.8, TIGR).

3. Results

3.1. Active components and target of XZPs in the treatment of HMG

According to the target information of active ingredients in TCMSP and TCMID database, combined with STP and superspeed target prediction results, a total of 123 targets of active ingredients in XZP were collected. Subsequently, by searching GeneCards, DisGeNET, and OMIM databases, 4656 targets of HMG were obtained. By matching drug-related targets with disease-related targets, 99 possible targets of XZP in treating HMG were obtained (Fig. 1a), and the active ingredient disease target network was further constructed (Fig. 1b). Sort according to the degree value, the top 10 active components were quercetin, luteolin, kaempferol, nobiletin, stigmasterol, isorhamnetin, isorhamnetin, β-Sitosterol, naringenin, pelargonidin, and aloe-emodin.

Subsequently, we constructed the PPI of 99 possible targets of XZPs in treating HMG through the STRING database (Fig. 1c). The PPI network consists of 99 nodes and 991 edges. After topological analysis of the targets (Fig. 1d and e), the core targets obtained include epidermal growth factor receptor (EGFR), interleukin 6 (IL6), vascular endothelial growth factor A (VEGFA), caspase 3 (CASP3), vascular endothelial growth factor A (VEGF), Mitogen-activated protein kinase 8 (MAPK8), Myc proto-oncogene protein (MYC), estrogen receptor (ESR1), G1/s-specific cyclin-D1 (CCND1), proto-oncogene c-fos (FOS), Receptor tyrosine-protein kinase erbB-2 (erbB2) and so on.

3.2. GO and KEGG pathway of XZPs in the treatment of HMG

We performed GO enrichment analysis of the biological process for 99 targets, with $p < 0.05$ as the screening criterion, 1338 items related to HMG were obtained, of which the closely related items include (Fig. 2a): response to a steroid hormone, response to xenobiotic stimulus, response to acid chemical, response to ketone (GO:1901654), response to the metal ion. Therefore, we speculate that XZP plays an anti-HMG role mainly through the above biological processes. In addition, 17 HMG-related pathways were obtained by KEGG pathway enrichment analysis (Fig. 2b), including MAPK, HIF-1, p53, Ras, ErbB, FoxO (Fig. 2c), and NF-kappa B signaling pathway (Fig. 2d). Based on those pathways above, the anti-HMG effect of the XZP may be the result of a complex multi-pathway synergetic effect.

3.3. Safety evaluation of XZP intervention in HMG mice

To evaluate the safety of the XZP in the treatment of HMG, we measured the levels of indexes of various organs in HMG mice. As shown in Fig. 3a, after 30 days of treatment, the Uterus and Spleen indexes of mice in the HMG group were markedly enhanced ($P < 0.05$), and the kidney and liver indexes were distinctly lowered ($P < 0.05$) compared with the control group. Simultaneously, compared with the HMG model group, the Uterus and Spleen indexes of each XZP treatment group were notably suppressed ($P < 0.05$), and the kidney and liver indexes were boosted ($P < 0.01$). The results indicate that the XZP improved the organ indexes in the Uterus, Spleen, kidney, and liver in HMG mice.

In addition, we used liver histopathological examination to further evaluate whether XZP intervention has hepatotoxicity. As

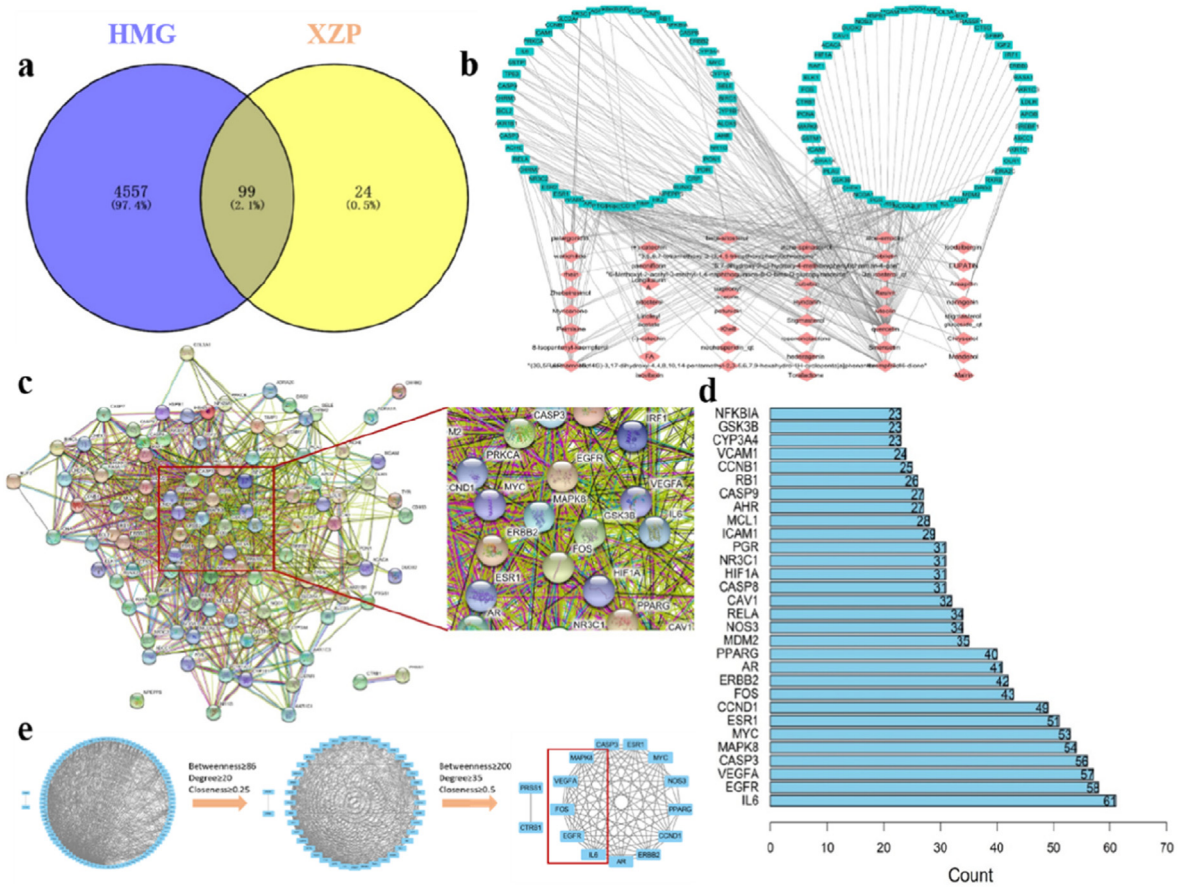

Fig. 1. Network pharmacology analysis of XZP in treating HMG. a, The Venn diagram of the targets both in HMG and XZP; b, Active ingredient - target network; c, The PPI network of 89 nodes; d, Topological analysis of HMG targets treated by XZP; e, The core target of XZP for HMG.

shown in Fig. 3b, results of the histopathologic analysis indicated that the liver organs had no obvious morphologic difference between XZP-treated HMG mice (1.8, 0.9, and 0.45 mg/g/d) and HMG model mice (Fig. 3b). Compared with the normal group, there was no abnormal change in liver tissue in each XZP dose group. The structure of hepatic lobules was normal, and the hepatocytes were distributed like cords, without swelling, steatosis, ballooning degeneration, and necrosis. There were sporadic inflammatory cells in the liver parenchyma and a few multinuclear cells in the hepatic lobules (Fig. 3b).

3.4. XZP ameliorated serum hormone levels and protected mammary gland tissue in HMG mice

To evaluate the anti-HMG effect of XZP, we measured the levels of serum sex hormones and pathological changes of the mammary gland in HMG mice. As shown in Fig. 4a, the serum levels of E2, P, LH, and FSH were measured by ELISA. The results showed that the levels of E2 and FSH in the model group were significantly higher than those in the normal control group ($P < 0.0001$); Compared with the HMG model group, the E2 levels of tamoxifen group, XZP low, medium, and high dose groups were significantly lower ($P < 0.0001$, 0.01, 0.001, 0.0001). In addition, ELISA results also showed that compared with the normal control group, the expression of P and LH in the HMG group was significantly lower ($P < 0.0001$); meanwhile, the expressions of P and LH in the tamoxifen group, XZP middle, and high dose group were significantly increased ($P < 0.0001$, 0.01, 0.0001).

As shown in Fig. 4b, the histopathological analysis showed that in the control group, lobules and acini showed no apparent hyperplasia. However, the mammary gland tissue of the HMG group showed obvious hyperplasia, lobules, acini increased, mammary duct dilation, and cavity secretion increased. Interestingly, after tamoxifen and XZP intervention, the proliferation of mammary lobules and the number of acini in HMG mice were significantly reduced. In addition, our study showed that the pathological improvement of breast hyperplasia was positively correlated with the dose of XZP. These results indicate that XZP has a therapeutic effect on HMG mice induced by estrogen and progesterone.

3.5. Screening results of different metabolites

By setting the thresholds of VIP, FC, and P ([VIP>1.0 and FC > 1.5] or [FC < 0.667 and P < 0.05]), the metabolites of four groups were analyzed, and 654 different metabolites were screened out. Among them, the number of different metabolites between the HMG model group and the normal group was 41, the number of different metabolites between the XZL group and HMG model group was 26, the number of different metabolites between the XZM group and HMG model group was 55, and the number of different metabolites between XZH group and HMG model group was 70 (Fig. 5a and b). Among the different metabolites between the HMG model group and the normal group, 18 metabolites intersected with three groups of XZP intervention (Fig. 5b): Cholesterol arachidonate, 19-Nortestosterone, Naringeninchalcone, Taurocholic acid, Tauro-alpha-Muricholic acid sodium salt, Glycocholic acid, Stevioside 4-

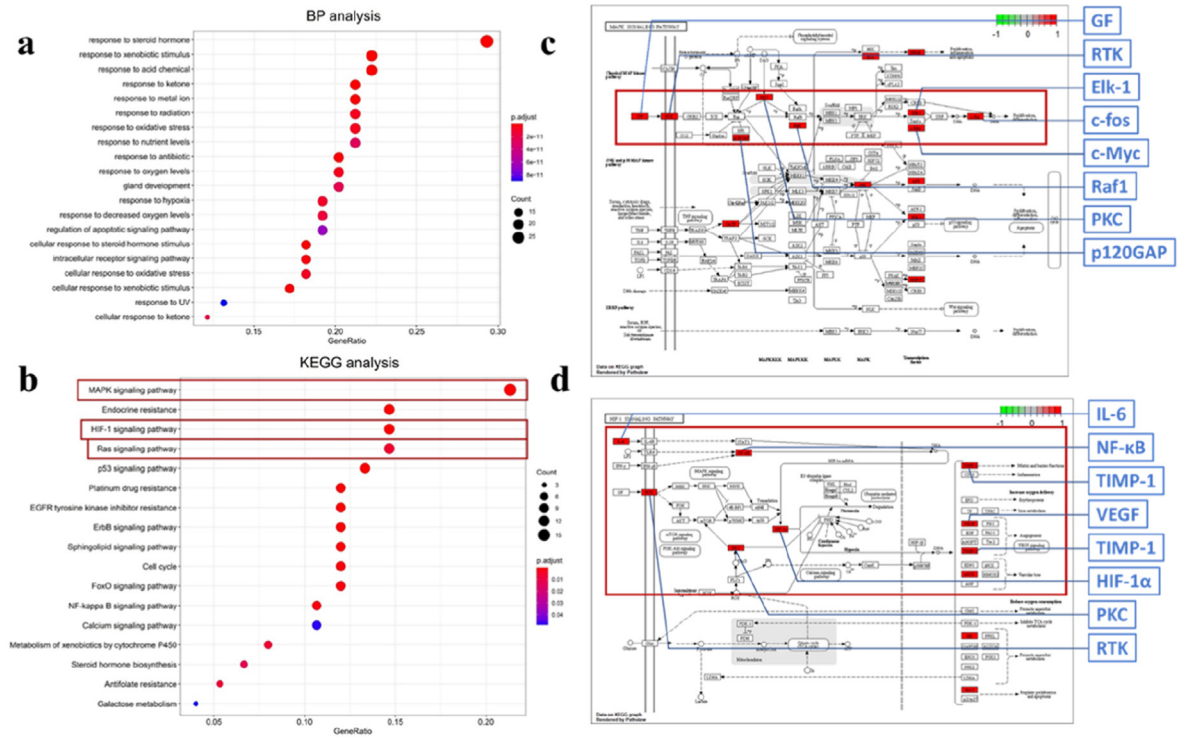

Fig. 2. GO biological process and KEGG pathway of XZPs in the treatment of HMG. a, The biological process (BP) of XZP for hyperplasia of mammary glands (HMG); b, The pathways of XZP in the treatment of HMG; The Key pathway (MAPK pathway, c) and (HIF-1 pathway, d) of XZP in the treatment of HMG.

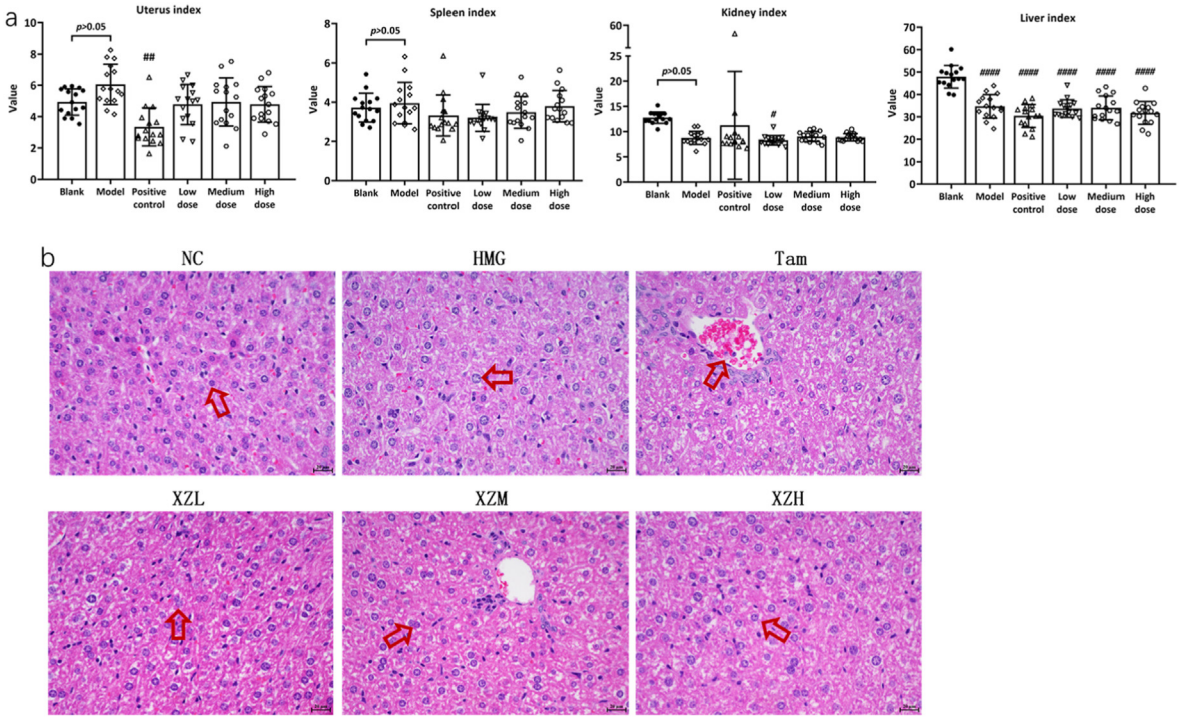

Fig. 3. Safety evaluation of XZP intervention in HMG mice. a, The levels of indexes of various organs in HMG mice.; b, The liver histopathological examination of HMG mice treated with XZP (HE staining, × 10). #$P < 0.05$,###$P < 0.001$,####$P < 0.0001$ vs normal control group; *$P < 0.05$,**$P < 0.01$,***$P < 0.001$ vs HMG model group.

Hydroxyindole, 23-Nordeoxycholic acid, 17α-Methyl-androstane-3-hydroxyimine-17β-ol, 13-HPODE, 6-[2-(2H-1,3-benzodioxol-5-yl) ethyl]-4-methoxy-2H-pyran-2-one, 3-(3-furyl methylidene)-1,5-dioxaspiro[5.5]undecane-2,4-dione, (11E,15Z)-9,10,13-trihydroxy octadeca-11,15-dienoic acid, 2-(14,15-Epoxyeicosatrienoyl) glycerol, Eicosapentaenoic acid, and Isotretinoin, 3-(2-thienyl)cinnoline-4-carboxylic acid. In addition, we used a volcano map and cluster map to display the metabolites of different groups. As shown in

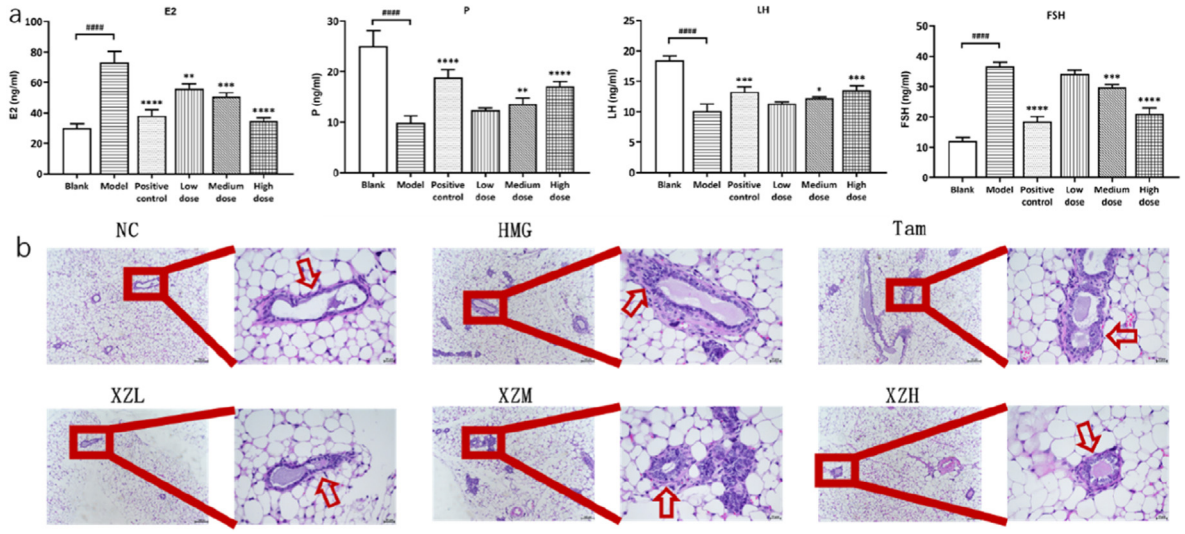

Fig. 4. Anti-HMG activity evaluation of XZP intervention in HMG mice. a, Effects of XZP on the E2, P, LH, and FSH levels in serum of mice; b, Pathological morphology of mammary gland tissue (HE staining, × 10, × 40). #$P < 0.05$,###$P < 0.001$,####$P < 0.0001$ vs normal control group; *$P < 0.05$,**$P < 0.01$,***$P < 0.001$ vs HMG model group.

Fig. 5c, compared with the normal group, the expression of most metabolites was up-regulated in the HMG group, while the expression of metabolites was down-regulated more significantly in the Xiaozheng pill groups. As shown in Fig. 5d, compared with the HMG model group, the metabolites of the XZP intervention group could be significantly aggregated, which further confirmed that XZP could significantly improve the metabolites of mice.

3.6. Functional analysis of different metabolites

Pathway enrichment analysis can determine the most important metabolic pathways involved in the differential metabolites, and then determine the main biological functions of the differential metabolites. As shown in Fig. 6, compared with the normal group, the main pathways involved in differentially expressed metabolites in the HMG model group include Primary bile acid biosynthesis, Cholesterol metabolism, and bile secretion; Compared with the HMG group, the metabolites in the XZL group mainly participate in metabolic pathways; Compared with the HMG group, the main pathways involved in different metabolites in the XZH group include primary bile acid biosynthesis, cholesterol metabolism, bile secretion, etc; Compared with the HMG model group, the differentially expressed metabolites in the XZH group are closely related to metabolic pathways and HIF-1 signaling pathways.

3.7. XZP attenuated ERα, ERβ, and PR expression in HMG mice

To investigate the regulation mechanism of XZP on E2 and P in HMG mice, we further studied the expression of ERα, ERβ, and PR in the breast tissue of HMG mice. As shown in Fig. 7, The expression of ERα, ERβ, and PR was observed in the six groups. Compared with that in the normal group, the expression of ERα, ERβ, and PR was increased in the breast tissue of mice with HMG. After 30 days of XZP treatment, the expression of ERα, ERβ, and PR in the breast tissue IHC was decreased. Especially, the treatment with 1.8 and 0.9 mg/g XZP significantly decreased the expression of ERα, ERβ, and PR ($p < 0.01$).

3.8. XZP inhibits the expressions of Raf1, ERK1/2, ELK, HIF-1α, VEGFA, and bFGF in breast tissue of HMG mice

As shown in Fig. 8a, compared with the normal control group, the expression of *p*-Raf1, Raf1, *p*-ERK1/2, ERK1/2, *p*-Raf1/Raf1, *p*-ERK/ERK, and ELK in the HMG model group were significantly increased ($P < 0.01$). After 30 days of treatment, the expression of *p*-Raf1, Raf1, *p*-ERK1/2, ERK1/2, ELK, and the ratios of *p*-Raf1/Raf1, *p*-ERK/ERK was decreased, especially in the high dose group of XZP, these expressions decreased significantly ($P < 0.05$).

At the same time, the angiogenesis-related proteins HIF-1α, VEGFA, and bFGF in the breast tissue of each group were detected. As shown in Fig. 8b, compared to the normal group, the protein levels of HIF-1α, VEGFA, and bFGF in the model group were significantly higher ($P < 0.0001$). Importantly, 30 days after XZP intervention, the expression of the proteins HIF-1α and bFGF were significantly decreased at various doses of XZP (Fig. 6b, $P < 0.01$). Additionally, the protein expression of VEGFA in the XZP groups decreased, although the difference was not statistically significant. These results indicate that XZP treatment may regulate the Raf-ERK-ELK and HIF-1α/bFGF signaling pathways in HMG mice.

4. Discussion

Network pharmacology can predict the target profile and pharmacological action of herbal medicine or traditional Chinese medicine formula.[25] In the current study, we used the method of network construction to explore the target of XZP in the treatment of HMG. The results showed that the main therapeutic targets of XZP for HMG included IL-6, EGFR, VEGFA, mapk8, ER, and HER-2. This is consistent with previous studies,[26–28] reflecting the clinical advantages of XZP in treating HMG. Network pharmacological analysis further concluded that the key pathways of XZP in the treatment of HMG include the HIF-1 signal pathway, MAPK signal pathway, RAS signal pathway, and so on. Previous studies have confirmed that compared with normal breast tissue, the microvessel density of breast hyperplasia tissue increased significantly, and the expression of HIF-1α and VEGF also increased significantly ($P < 0.05$).[29] Ras family proteins include H-ras, N-ras, and K-ras. Studies have found that overexpression of H-ras and N-ras can induce cell proliferation and phenotypic transformation of human

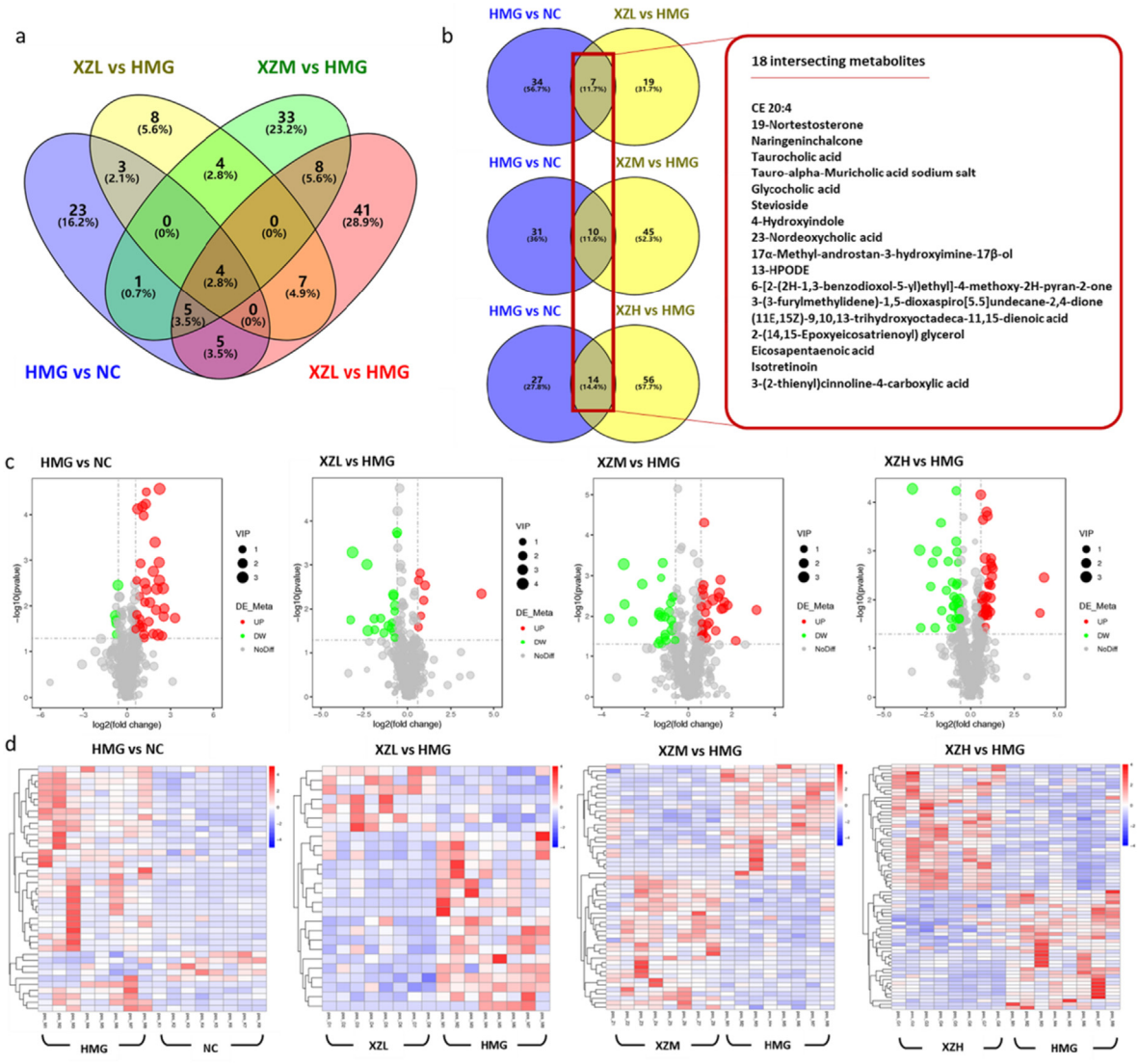

Fig. 5. The differentially expressed metabolites in each group. a and b, Venn diagram of different metabolites among different groups; c, Volcanic maps of different metabolites. The abscissa represents the log2 fold change of metabolites in different groups, and the ordinate represents the different significance levels (- log10 P). Each point in the volcanic map represents a metabolite. The significantly up-regulated metabolite is represented by a red dot, the significantly down-regulated metabolite is represented by a green dot, and the size of the dot represents the VIP value. d, V Cluster analysis of different metabolites. The vertical clustering of samples and the horizontal clustering of metabolites are shown in the thermogram. The shorter the cluster branch, the higher the similarity.

breast epithelial cell mcf10a.[30] In addition, through the analysis of 171 cases of breast tissue sections, found that the expression of p21 Ras gradually increased from normal breast epithelium to a common type of epithelial hyperplasia, and then to atypical breast epithelial hyperplasia.[31] In conclusion, the results of network pharmacology analysis suggest that the therapeutic effect of XZP on HMG may be closely related to regulating the expression of key targets in HIF-1 and RAS signaling pathways such as EGFR, VEGFA, ER, and HER-2.

Then, we verified the authenticity of the network pharmacology analysis results through animal experiments and further revealed the mechanism of XZP in treating HMG. As we all know, the increase of estrogen levels in the body can promote the proliferation of breast cells.[32] Long-term high E2 stimulation destroys the balance of breast tissue proliferation, leading to the expansion of the mammary duct, the increase of adenoma and acinus, and then leading to pathological breast hyperplasia.[33] Because of the above mechanism of HMG, we used estradiol benzoate and P to induce the HMG mice model.[34,35] Our results showed that the serum E2 level of HMG model mice increased significantly. In addition, with the increase in E2 level, serious pathological changes appeared in breast tissue, and different doses of XZPs could improve the hormone level, biochemical indexes, and pathological changes of HMG model animals to varying degrees. We further confirmed the safety of XZP by analyzing the organ index and liver tissue morphology of mice in each group. The expression level of ER and PR in breast hyperplasia tissue was higher than that of normal breast tissue.[36] Consistent with previous studies, our results showed that compared with the HMG model group, the expression levels of Erα, Erβ, and PR in mammary gland tissue of mice in each dose group of XZP intervention were significantly decreased, especially in middle and high doses of XZP group, which effect was better than that of tamoxifen group.

Metabolomics technology can quantitatively analyze all the metabolites in the organism by measuring the endogenous metabolites in the blood, which can show the changes of small

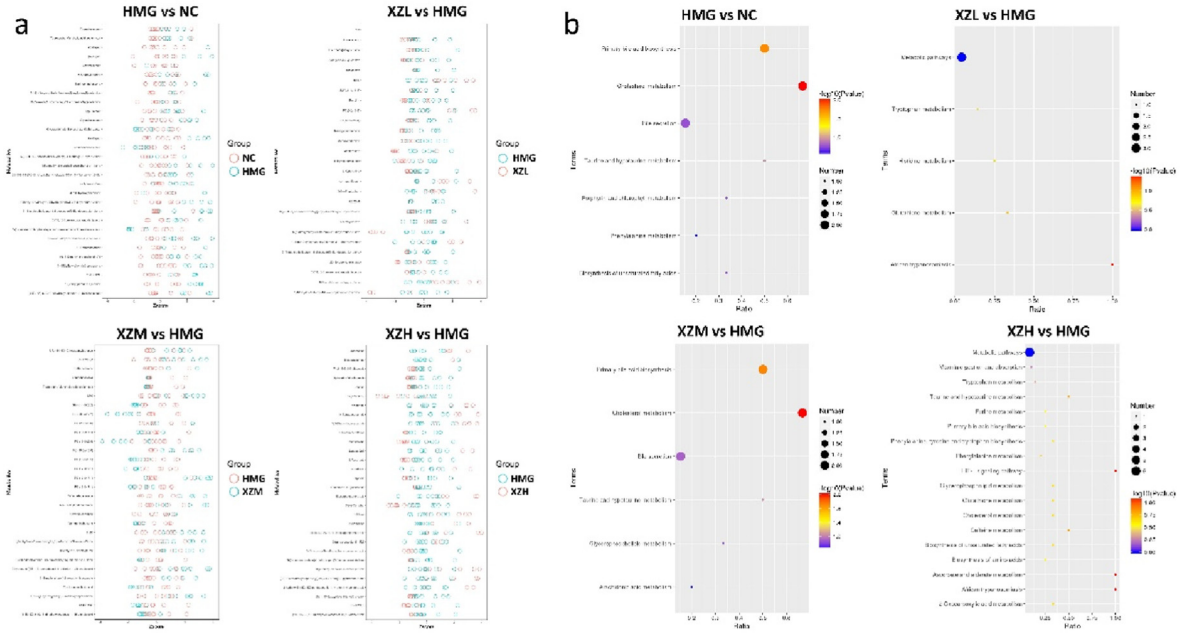

Fig. 6. Functional analysis of different metabolites. a, Z-score analysis chart; b, KEGG bubble chart.

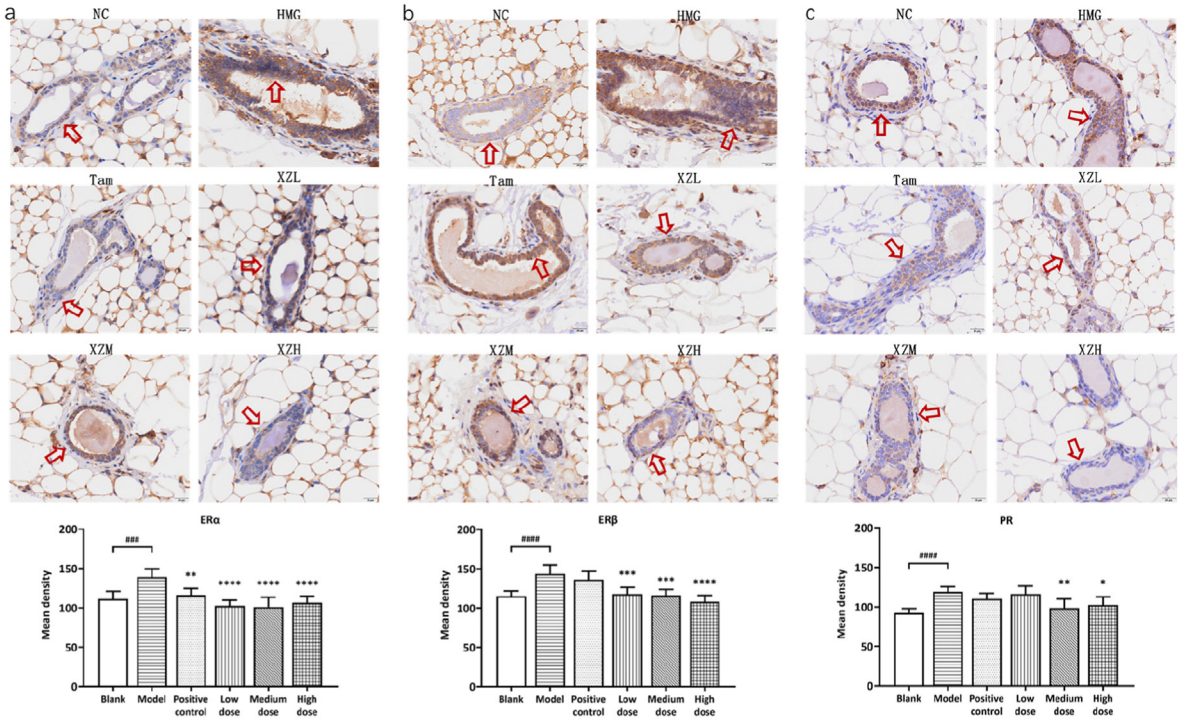

Fig. 7. XZP attenuated ERα, ERβ, and PR expression in HMG mice (× 40). a, The expression level of ERα; b, The expression level of ERβ; c, The expression level of PR. #$P < 0.05$, ###$P < 0.001$, ####$P < 0.0001$ vs normal control group; *$P < 0.05$, **$P < 0.01$, ***$P < 0.001$ vs HMG model group.

molecule metabolites of substrates and products of various metabolic pathways in different states.[37] Through the changes in the metabolite map, we can better understand the pathological state of the disease and the metabolic mechanisms of drugs. Our metabolomics results show that XZP can significantly improve the metabolites of mice. Compared with the HMG model group, the differentially expressed metabolites in the XZP group are closely related to metabolic pathways, primary bile acid biosynthesis, cholesterol metabolism, and the HIF-1 signaling pathway. Studies have shown that the HIF pathway plays a core role in the cellular mechanism triggered by hypoxia.[38] HIF-1α, a transcription factor, plays an active role in specific hypoxia and is widely involved in the regulation of various cellular signaling pathways.[39] The oxygen state can regulate the stability of HIF-1 family proteins.[40] Research has shown that HIF-1α plays a unique role in tumor development, with HIF and its subtypes overexpressed in most human cancers.[41]

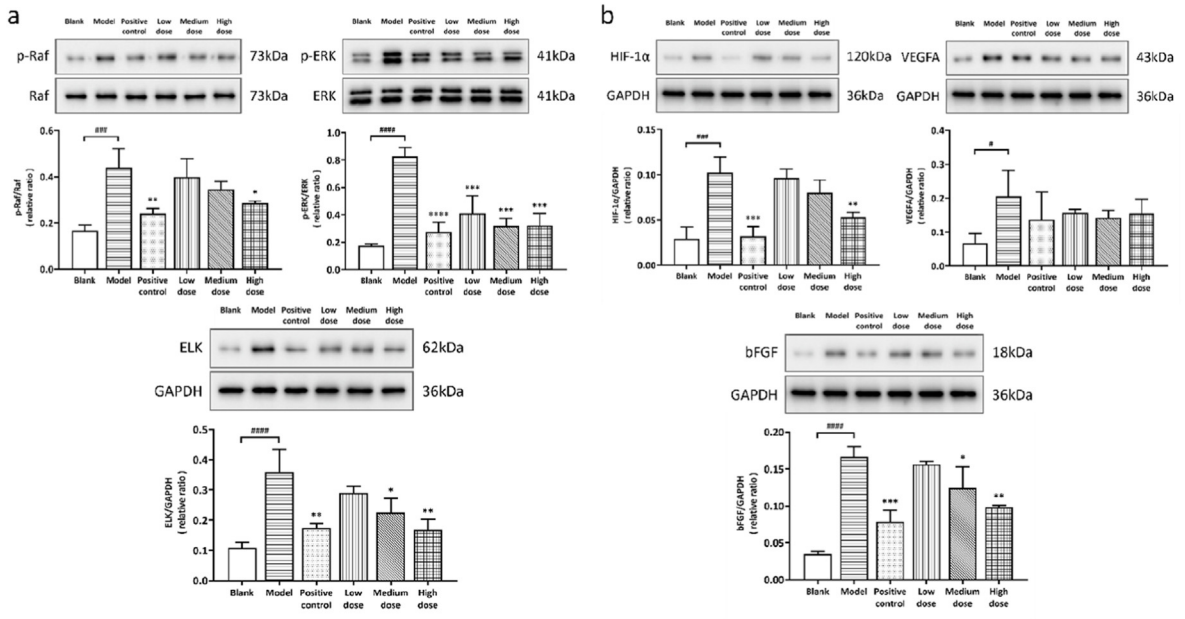

Fig. 8. XZP modulated proliferation-related and angiogenesis-related proteins in HMG mice. a, Expression changes of proliferation-related proteins; b, Expression changes of angiogenesis-related proteins. #$P < 0.05$, ###$P < 0.001$, ####$P < 0.0001$ vs normal control group; *$P < 0.05$, **$P < 0.01$, ***$P < 0.001$ vs HMG model group.

In summary, based on the results of network pharmacology research and metabolomics, we speculate that XZP may exert anti-HMG effects by regulating the Ras and HIF-1 signaling pathways to inhibit breast epithelial cell proliferation and angiogenesis.

Then, to further study its anti-HMG mechanism, we combined it with the results of network pharmacology, selected cell proliferation, and angiogenesis-related pathways to systematically verify the mechanism. Raf and ERK are the key proteins in the Ras-Raf-ERK signaling pathway, belonging to one of the MAPK pathways. This pathway transmits extracellular signals into the nucleus through cell membrane receptors, thus mediating the expression of specific proteins in cells and participating in the regulation of cell proliferation, differentiation, and other functions. Under normal conditions, RAS binding to guanosine diphosphate is inactivated, while Ras binding to guanosine triphosphate (GTP) becomes activated when stimulated by exogenous guanine nucleotide exchange factor (GEF). GTP Ras phosphorylates Raf, causing downstream ERK activation. ERK proteins include ERK1 and ERK2 proteins, which have similar functions and are activated in parallel in vivo.[42,43] ELK is a common downstream target molecule of ERKs and MAPK pathway, which is mainly activated by MAPK-mediated mitogen or growth factor stimulation.[44] Phosphorylation of ERK1/2 can further catalyze the phosphorylation of ELK and other transcription factors.[45] In the current study, we found that the ratio of *p*-Raf/Raf, the ratio of *p*-ERK/ERK, and the expression of ELK increased significantly in the breast tissue of HMG mice; Interestingly, the ratio of *p*-Raf/Raf, the ratio of *p*-ERK/ERK and the expression of ELK protein were significantly decreased after the intervention of XZP, which is consistent with our network pharmacology results, further indicating that XZP may exert a therapeutic effect on HMG by inhibiting cell proliferation through the Raf-ERK-ELK pathway.

HIF-1α is widely present in mammalian cells and plays an important regulatory role in cell growth and proliferation. VEGF can not only increase the permeability of vascular endothelial cells but also promote the formation of new blood vessels. In addition, bFGF is one of the direct inducers of angiogenesis and plays a key role in the process of regulating angiogenesis. It can promote the regeneration of epidermal and endothelial cells, and induce the division of vascular endothelial cells. Some vascular factors in breast tissue may be activated, which directly or indirectly induces the proliferation of blood vessels in local breast tissue, leading to the occurrence of HMG.[46] The Western blot results showed that consistent with the results of metabolomics and network pharmacology analysis, the expression of HIF-1α, VEGFA, and bFGF in the breast tissue of HMG mice was significantly increased; In addition, after different doses of XZP intervention, the expression levels of HIF-1α and bFGF were significantly reduced. This further confirms that XZP may exert anti-HMG effects by affecting the angiogenesis-related HIF-1α/VEGFA pathway, but the interaction between HIF-1α and VEGFA has not been studied in this study. In addition, bFGF is an upstream protein of Ras/Raf.[47] Based on the research results of proliferation-related pathways, we speculate that XZP can eliminate abnormal breast hyperplasia by inhibiting cell apoptosis and angiogenesis, which may be related to the regulation of Raf/ERK/ELK and HIF-1α/bFGF signaling pathways in HMG mice.

5. Conclusions and outlook

In summary, we systematically studied the pharmacological mechanism of XZP in the treatment of HMG through network pharmacology and mouse experiments. XZP treatment may improve the morphology of HMG and elimination of abnormal hyperplasia through inhibition of Apoptosis and Angiogenesis via regulating the Raf/ERK/ELK and HIF-1α/bFGF signaling. In addition, the XZP may also regulate the metabolites related to HMG. These results may suggest the potential of the XZP in preventing the development of HMG and indicate that XZP could be a new therapeutic strategy for the treatment of HMG, which needs to be further confirmed in cell experiments and clinical trials.

Author contributions

Xiaohua Pei and Yingyi Fan designed the experiments; Tian An and Yufei Liu wrote the manuscript. Tian An, Yufei Liu, and Hong Yu performed the experiments. Tian An and Yufei Liu analyzed the data. All authors reviewed the manuscript.

Funding

This work was financially supported by grants from the Horizontal Scientific Research Project of Lei Yunshang Group, and the independent subject graduate student projects of Beijing University of Chinese Medicine (2019-XS-ZB12).

Conflicts of interest

The authors declare no conflicts of interest concerning the authorship and/or publication of this paper.

Acknowledgments

Not applicable.

Appendix A. Supplementary data

Supplementary data to this article can be found online at https://doi.org/10.1016/j.jtcme.2023.05.002.

Abbreviations

(HMG)	hyperplasia of mammary glands
(E2)	Estradiol
(P)	Progesterone
(ERα)	Estrpgen receptor α
(PR)	Progesterone receptor
(ERβ)	Estrpgen receptor β
(TAM)	Tamoxifen
(TCMSP)	Traditional Chinese medicine systems pharmacology database and analysis platform
(TCMID)	Traditional Chinese medicine integrated database
(STP)	Swiss target prediction
(OMIM)	Online Mendelian Inheritance in Man
(OB)	Oral bioavailability
(DL)	Drug-likeness
(DC)	Degree centrality
(CC)	Closeness centrality
(DAVID)	The Database for Annotation, Visualization, and Integrated Discovery
(KEGG)	Kyoto encyclopedia of genes and genomes
(BC)	Betweenness centrality
(PPI)	Protein-protein interaction
(BP)	Biological process
(SPF)	Specific pathogen-free
(BUCM)	Beijing University of Chinese Medicine
(NC)	normal group
(Tam)	Tamoxifen-treated control group
(XZH)	XZP high dose-treated group
(XZM)	XZP medium dose-treated group
(XZL)	XZP low dose-treated group
(FSH)	Follicle-stimulating hormone
(LH)	Luteinizing hormone
(PRL)	Prolactin
(LC-MS)	Liquid chromatography mass spectrometry
(Raf)	Principal component analysis (PCA). RAF proto-oncogene serine/threonine-protein kinase
(ERK)	extracellular signal-regulated kinase
(ELK)	ETS domain-containing protein
(MAPK)	mitogen-activated protein kinase
(GTP)	guanosine triphosphate
(GEF)	guanine nucleotide exchange factor
(LDL)	low-density lipoprotein

References

1. Li P, Huang J, Wu H, Fu C, Li Y, Qiu J. Impact of lifestyle and psychological stress on the development of early onset breast cancer. *Medicine (Baltim)*. 2016 Dec;95(50), e5529.
2. Wei S, Zhou X, Niu M, et al. Network pharmacology exploration reveals the bioactive compounds and molecular mechanisms of Li-Ru-Kang against hyperplasia of mammary gland. *Mol Genet Genom*. 2019 Oct;294(5):1159–1171.
3. Jiang M, Liang Y, Pei Z, et al. Diagnosis of breast hyperplasia and evaluation of RuXian-I based on metabolomics deep belief networks. *Int J Mol Sci*. 2019 May 28;20(11):2620.
4. Ma D, Liu G, Zhang X, Zhang Q, Gao T, Liu M. Massage treatment of hyperplasia of mammary glands: a protocol for a systematic review and meta-analysis. *Medicine (Baltim)*. 2020 Dec 24;99(52), e23601.
5. Li X, Shi G. Therapeutic effects and mechanism of ferulic acid and icariin in mammary gland hyperplasia model rats via regulation of the ERK pathway. *Ann Transl Med*. 2021 Apr;9(8):666.
6. Adeniji-Sofoluwe AT, Obajimi GO, Obajimi MO. Pregnancy related breast diseases in a developing African country: initial Sonographic Evaluation. *Pan Afr Med J*. 2015 Mar 13;20:239.
7. Lilleborge M., Falk R.S., Sørlie T., Ursin G., Hofvind S. Can breast cancer be stopped? Modifiable risk factors of breast cancer among women with a prior benign or premalignant lesion. Int J Cancer.2021 Sep 15;149(6):1247-1256.
8. You Z, Sun J, Xie F, et al. Modulatory effect of fermented papaya extracts on mammary gland hyperplasia induced by estrogen and progestin in female rats. *Oxid Med Cell Longev*. 2017;2017, 8235069.
9. Gao H, Yang C, Fan J, Lan L, Pang D. Hereditary and breastfeeding factors are positively associated with the aetiology of mammary gland hyperplasia: a case-control study. *Int Health*. 2021 Apr 27;13(3):240–247.
10. Polat AK, Soran A, Kanbour-Shakir A, Menekse E, Levent Balci F, Johnson R. The role of molecular biomarkers for predicting adjacent breast cancer of Atypical Ductal Hyperplasia diagnosed on core biopsy. *Cancer Biomarkers*. 2016 Sep 26;17(3):293–300.
11. Wang R, Li B, Lam SM, Shui G. Integration of lipidomics and metabolomics for in-depth understanding of cellular mechanism and disease progression. *J Genet Genomics*. 2020 Feb 20;47(2):69–83. https://doi.org/10.1016/j.jgg.2019.11.009. Epub 2019 Dec 18. PMID: 32178981.
12. Li X, Xin P, Wang C, Wang Z, Wang Q, Kuang H. Mechanisms of traditional Chinese medicine in the treatment of mammary gland hyperplasia. *Am J Chin Med*. 2017;45(3):443–458. https://doi.org/10.1142/S0192415X17500276.Epub.2017.Mar.30. PMID: 28359197.
13. Gong Lei, Zhao Xiaoli, Di Liuqing. Etc establishment of HPLC fingerprint of Xiaozheng pill and its methodological study [C]//Traditional Chinese medicine preparations branch of China association of Chinese medicine, professional committee of traditional Chinese medicine of world federation of Chinese medicine societies. *Proceedings of the "Good Doctor Cup" Forum on Innovation and Development of Traditional Chinese Medicine Preparations*. 2013;(Part 2):10.
14. Liu Yang, Wang Wenbin, Miao Wenqing, Huang Ming, Chen Daping. Clinical study on Xiaozheng pill in the treatment of hyperplasia of mammary glands. *Information of traditional Chinese medicine*. 2016;33(4):93–96.
15. Wang Jiangang, Qi Chen, Yan zhangren, Wang Wanchun. Clinical observation of Xiaozheng pill in the treatment of hyperplasia of mammary glands. *Modern distance education of traditional Chinese medicine*. 2018;16(6):118–120.
16. Jacob M, Lopata AL, Dasouki M, Abdel Rahman AM. Metabolomics toward personalized medicine. *Mass Spectrom Rev*. 2019 May;38(3):221–238.
17. Adeola HA, Papagerakis S, Papagerakis P. Systems biology approaches and precision oral health: a circadian clock perspective. *Front Physiol*. 2019 Apr 16;10:399.
18. Johnson CH, Ivanisevic J, Siuzdak G. Metabolomics: beyond biomarkers and towards mechanisms. *Nat Rev Mol Cell Biol*. 2016 Jul;17(7):451–459.
19. Liu Y, An T, Wan D, Yu B, Fan Y, Pei X. Targets and mechanism used by cinnamaldehyde, the main active ingredient in cinnamon, in the treatment of breast cancer. *Front Pharmacol*. 2020 Dec 9;11, 582719.
20. Miao mingsan, Wen Yajuan, Ming Bai, et al. Preparation standard of mammary gland hyperplasia animal model. *Chinese Journal of experimental prescriptions*. 2017;23(24):17–22.
21. Xu Shuyun. *Pharmacological Experimental Methodology*. third ed. [M]. Beijing: People's Health Publishing House; 2002, 01.
22. Jia Y, Liu X, Jia Q, et al. The anti-hyperplasia of mammary gland effect of protein extract HSS from Tegillarca granosa. *Biomed Pharmacother*. 2017 Jan;85:1–6.
23. Mo FF, An T, Zhang ZJ, et al. Tang xiao ke granule play an anti-diabetic role in diabetic mice pancreatic tissue by regulating the mRNAs and MicroRNAs associated with PI3K-akt signaling pathway. *Front Pharmacol*. 2017 Nov 1;8:795.
24. Wang C, Liu C, Wang M, et al. UPLC-HRMS-Based plasma metabolomic profiling of novel biomarkers by treatment with KDZI in cerebral ischemia reperfusion rats. *Molecules*. 2018 May 30;23(6):1315.
25. Wei S, Zhou X, Niu M, et al. Network pharmacology exploration reveals the bioactive compounds and molecular mechanisms of Li-Ru-Kang against hyperplasia of mammary gland. *Mol Genet Genom*. 2019 Oct;294(5):1159–1171. https://doi.org/10.1007/s00438-019-01569-5. Epub 2019 May 3. PMID: 31053932.
26. Gregory KJ, Roberts AL, Conlon EM, et al. Gene expression signature of atypical breast hyperplasia and regulation by SFRP1. *Breast Cancer Res*. 2019 Jun

27;21(1):76.
27. Longatto Filho A, Costa SM, Milanezi F, et al. Immunohistochemical expression of VEGF-A and its ligands in non-neoplastic lesions of the breast sampling-assisted by dynamic angiothermography. *Oncol Rep*. 2007 Nov;18(5):1201–1206.
28. Mao X, Qiao Z, Fan C, et al. Expression pattern and methylation of estrogen receptor α in breast intraductal proliferative lesions. *Oncol Rep*. 2016 Oct;36(4):1868–1874.
29. Bluff JE, Menakuru SR, Cross SS, et al. Angiogenesis is associated with the onset of hyperplasia in human ductal breast disease. *Br J Cancer*. 2009 Aug 18;101(4):666–672.
30. Yong HY, Hwang JS, Son H, et al. Identification of H-Ras-specific motif for the activation of invasive signaling program in human breast epithelial cells. *Neoplasia*. 2011 Feb;13(2):98–107.
31. Going JJ, Anderson TJ, Wyllie AH. Ras p21 in breast tissue: associations with pathology and cellular localisation. *Br J Cancer*. 1992 Jan;65(1):45–50.
32. Zhang JF, Liu J, Gong GH, Zhang B, Wei CX. Mongolian medicine RuXian-I treatment of estrogen-induced mammary gland hyperplasia in rats related to TCTP regulating apoptosis. *Evid Based Complement Alternat Med*. 2019 Mar 19;2019, 1907263.
33. Warner M, Wu WF, Montanholi L, Nalvarte I, Antonson P, Gustafsson JA. Ventral prostate and mammary gland phenotype in mice with complete deletion of the ERβ gene. *Proc Natl Acad Sci U S A*. 2020 Mar 3;117(9):4902–4909.
34. You Z, Sun J, Xie F, et al. Modulatory effect of fermented papaya extracts on mammary gland hyperplasia induced by estrogen and progestin in female rats. *Oxid Med Cell Longev*. 2017;2017, 8235069.
35. Chen T, Li J, Chen J, Song H, Yang C. Anti-hyperplasia effects of Rosa rugosa polyphenols in rats with hyperplasia of mammary gland. *Environ Toxicol Pharmacol*. 2015 Mar;39(2):990–996.
36. Hilton HN, Clarke CL, Graham JD. Estrogen and progesterone signalling in the normal breast and its implications for cancer development. *Mol Cell Endocrinol*. 2018 May 5;466:2–14.
37. Xiaochen H, Shulan S, Jianming G, et al. Application and thinking of metabolomics in the research of some scientific problems of traditional Chinese medicine. *Chin Tradit Herb Drugs*. 2014;45(2):147–153.
38. McGettrick AF, O'Neill LAJ. The role of HIF in immunity and inflammation. *Cell Metabol*. 2020 Oct 6;32(4):524–536.
39. Yang H, Tan M, Gao Z, Wang S, Lyu L, Ding H. Role of hydrogen sulfide and hypoxia in hepatic angiogenesis of portal hypertension. *J Clin Transl Hepatol*. 2023 Jun 28;11(3):675–681.
40. Li Y, Zhang MZ, Zhang SJ, et al. HIF-1α inhibitor YC-1 suppresses triple-negative breast cancer growth and angiogenesis by targeting PlGF/VEGFR1-induced macrophage polarization. *Biomed Pharmacother*. 2023 May;161, 114423.
41. Jing X, Yang F, Shao C, et al. Role of hypoxia in cancer therapy by regulating the tumor microenvironment. *Mol Cancer*. 2019 Nov 11;18(1):157.
42. Cagnol S, Chambard JC. ERK and cell death: mechanisms of ERK-induced cell death–apoptosis, autophagy and senescence. *FEBS J*. 2010 Jan;277(1):2–21.
43. Xue W, Pinghu Z. Research progress of Ras/Raf/MEK/ERK signaling pathway involved in autophagy regulation. *J China Pharm Univ*. 2017;48(1):110–116.
44. Kasza A. Signal-dependent Elk-1 target genes involved in transcript processing and cell migration. *Biochim Biophys Acta*. 2013 Oct;1829(10):1026–1033.
45. Yixuan W, Ke W, Shu Z. Research progress of Elk-1 regulating skeletal system function. *Chin J Osteoporos*. 2020;26(12):1857–1860.
46. Liyan G, Jingru X, Qi L, et al. Effect of Jiedu Capsule on the expression of VEGF and bFGF in rats with hyperplasia of mammary glands. *Chinese Journal of traditional Chinese medicine*. 2016;34(7):1559–1562.
47. Haghighi F, Dahlmann J, Nakhaei-Rad S, et al. bFGF-mediated pluripotency maintenance in human induced pluripotent stem cells is associated with NRAS-MAPK signaling. *Cell Commun Signal*. 2018 Dec 5;16(1):96.